



## Full Length Article

## Calculations of selective Si epitaxial growth

Wenrui Chai<sup>a</sup>, Muthukumar Kaliappan<sup>b</sup>, Michael Haverty<sup>b</sup>, David Thompson<sup>b</sup>, Graeme Henkelman<sup>a,\*</sup><sup>a</sup> Department of Chemistry and the Oden Institute for Computational Engineering and Sciences, The University of Texas, Austin, TX 78712, United States<sup>b</sup> Chemistry CoE, New Markets and Alliances, Applied Materials, Santa Clara, CA 95054, United States

## ARTICLE INFO

## Keywords:

Selective epitaxial growth  
Dichlorosilane  
Density functional theory

## ABSTRACT

Dichlorosilane (DCS) is widely used in the semiconductor industry for selective epitaxial growth (SEG) of Si. Si SEG currently requires high temperatures, on the order of 800 °C; multiple approaches have been attempted to deposit Si at lower temperature, but no viable alternatives have been found. This failure is attributed to a poor understanding of the mechanisms and the underlying factors that determine Si growth. In this study, we investigate Si SEG using DCS and HCl on a crystalline silicon (c-Si) surface as compared to on SiO<sub>2</sub> using density functional theory. Our calculations of Si SEG reaction mechanisms illustrate three factors that contribute to selectivity. First is that surface passivation by Cl does not limit SEG growth on c-Si while it hinders nucleation on the SiO<sub>2</sub> surface. Second is that amorphous growth at nucleation sites on the SiO<sub>2</sub> surface is slower than epitaxial growth on c-Si. Third is that the low entropic cost of epitaxial growth on c-Si is important for selectivity. The mechanistic understanding from this investigation suggests that future searches for low-temperature SEG of Si could focus on SiH<sub>2</sub>R<sub>2</sub> like precursors.

## 1. Introduction

Evolving sub 10 nm semiconductor device architectures requires controlled growth of Si. Selective epitaxial growth (SEG) is an essential reaction for this down-scaling. [1] In the SEG process, the Si precursor is deposited selectively on the Si surface over a dielectric surface. The selectivity is attributed to differences in both the growth rate and the growth mechanism, where on the c-Si surface, a faster layer by layer growth is seen as compared to slower amorphous growth on the SiO<sub>2</sub> surface. Additionally, Si growth on the SiO<sub>2</sub> surface can be more easily etched than on c-Si, facilitating SEG on c-Si surfaces [2].

There are several silicon precursors for SEG, including silane [3], disilane [4], dichlorosilane [5] and dichlorosilane (DCS) [6]. DCS has a relatively low growth rate at about one tenth that of silane, which in turn is ten times slower than disilane. A recent study on the kinetics of deposition using these precursors suggests that the rate limiting step is desorption of H or Cl [7]. Though silane is capable of deposition at low temperature, SEG is only reported at 950 °C with silane [8]. DCS is widely used because it allows for a wide temperature range of deposition. Specifically, high quality material can be grown at temperatures as low as 750 °C while the reaction becomes mass transport limited at 950 °C [7]. In addition, DCS is more selective than other silicon sources, including silane [9]. In fact, when used together with silane, DCS

functions as an etching agent to provide selectivity [10,11]. Higher order silicon precursors that have more than three Si atoms can deposit at low temperature (< 600 °C) yet the resulting film is not epitaxial due to particle formation on the surface [12]. Disilane allows for growth at temperatures as low as 500 °C, yet the resulting surface is found to have defects [13]. Alternative techniques such as using an increased flow of HCl for selectivity leads to a linear decrease in SEG.1

While the search for a faster SEG reagent continues, the reaction mechanism and the origin of selectivity remains elusive. A recent study attributes the SEG to the difference in deposition barrier on different surfaces, yet it was unable to provide barriers that agree with experimental activation energies [14]. Hierlemann et al. proposed a single step reaction model for DCS:  $SiH_2Cl_2 \rightarrow Si * + 2HCl$ , [15] which has been validated in recent macroscale experimental studies [16], but no details of the SEG mechanism(s) were provided. The mechanism for higher order silane SEG is also unclear. It has been proposed that their deposition rate is higher because they do not depend on H desorption reactions, [17] but it is not clear why H desorption does not limit deposition by higher order silicon precursors. Three decades after adoption of CVD by DCS, no precursor that can deposit at lower temperature than DCS with comparable selectivity has been found. Hence, a theoretical investigation of the mechanism and atomic level features can provide insight into SEG and offer clues on how to design silicon

\* Corresponding author.

E-mail addresses: [chaiwenrui@utexas.edu](mailto:chaiwenrui@utexas.edu) (W. Chai), [muthukumar\\_kaliappan@amat.com](mailto:muthukumar_kaliappan@amat.com) (M. Kaliappan), [henkelman@utexas.edu](mailto:henkelman@utexas.edu) (G. Henkelman).

precursors that deposit Si at a higher rate, lower temperature, and with higher selectivity.

In this study, we use density functional theory (DFT) to provide energetics and reaction mechanisms for SEG. We show that SEG is not governed by a single factor and does not occur by a single mechanism. Rather, understanding SEG requires consideration of factors including surface passivation reactions and different growth mechanisms on multiple surfaces. We use the calculated free energy landscapes to address the factors that favor selectivity of SEG on Si over SiO<sub>2</sub>.

## 2. Methods

DFT calculations were conducted as implemented in the Vienna Ab-Initio Simulation Package [18–21]. Core electrons were described within the projected augmented wave framework; [22] valence electrons were described with a plane wave basis set up to an energy cutoff of 300 eV, which was appropriate for the soft oxygen pseudopotential used. The generalized gradient approximation in the form of the Perdew, Burke and Ernzerhof functional was used to model electronic exchange and correlation [23].

The Si slab used in this study was a supercell of a (4x4x4) cubic Si unit cell with 12 Å of vacuum, exposing the (1 0 0) surface. The atoms in the bottom 4 layers of the slab were constrained to their bulk geometries; all other atoms were relaxed. The box size was chosen to provide sufficient spacing between periodic images. Some reactions produce gas phase products that diffuse away from the reaction site so that a smaller supercell would result in periodic images interacting with each other. The Brillouin zone was sampled at the  $\Gamma$  point, which was found to be sufficient for the large-cell modeled.

SEG requires specific conditions including (1) temperatures around 850 °C (2) an H<sub>2</sub> atmosphere and (3) a clean surface. High temperature and an H<sub>2</sub> environment facilitate the release of surface oxygen atoms, but also passivates the Si surface and prevents further adsorption of oxygen-based moieties to the surface [24]. Accordingly, in this study we use a H terminated Si surface with surface SiH<sub>2</sub> groups on both sides of the slab (the A1 surface in Fig. 1) and determine the interactions with DCS. The 2 × 1 reconstructed surface terminated by (SiH)<sub>2</sub> groups was not used because it converts back to the A1 surface. Though this 2 × 1 reconstructed surface is a common model [25] and is stable in a H<sub>2</sub> environment, further hydrogenation by H<sub>2</sub> has a high barrier (shown in Fig. S15) and it is not stable in the presence of HCl. Fig. S16 shows that HCl breaks the surface Si-Si bond with a barrier of only 1 eV, producing the A4 surface in Fig. 1. This surface can be converted back to the A1 surface as shown in Fig. 3.

SiO<sub>2</sub> (1 1 1) surfaces with a hydrogen termination were modeled with a (2x2x2) supercell cleaved from (quartz/cristobalite) and considered for precursor interaction. Specifically, the reaction mechanisms of DCS with the Si/SiO<sub>2</sub> surfaces were determined.

Reaction pathways were calculated using the climbing image nudged elastic band method (CI-NEB) [26] with double nudging, [27] coupled in some cases with the dimer method [28]. For each band, 8 images were used, and increased to 14 when additional resolution was needed. Reaction free energies were calculated using DFT energies and entropies of all atoms participating in the reactions. Gas phase molecules were treated as ideal gases. Vibrations were treated as harmonic oscillators. The total entropy of adsorbed species were calculated using the Campbell-Sellers equation, [29]

$$S_{ad}(T) = 0.70S_{gas}(T) - 3.3R \quad (1)$$

The translational entropy was calculated using the Sakur-Tetrode equation, (Eq. (2)), and rotational entropies were calculated from rotational partition functions. In a transition from reactant to transition state, it was approximated that one mode was lost,

$$S_t = R \left[ \ln \left( \frac{(2\pi mkT)^{3/2} V}{h^3 N} \right) + 2.5 \right] \quad (2)$$

Values for N/V were taken from the literature [1], where the pressure of the anhydrous co-flow gas was set as 30 torr, and the ratio for H<sub>2</sub>, DCS and HCl are 230 : 0.9 : 1. By-products of reactions that are not in the co-flow gas have an assumed concentration of 1 ppb, including chlorosilane (CS), trichlorosilane (TCS), chlorosilanol (SiH<sub>2</sub>ClOH) and water. This is approximately the impurity ratio of reagent grade reactants. The reaction temperature was set at 800 °C.

## 3. Results and discussion

The most relevant reactions are shown in Figs. 1 and 2. These include reactions that passivate or activate the surfaces, and those that deposit Si onto the surface. Etching reactions and reactions of the aforementioned types with higher enthalpic barriers are not important for these results and are shown only in the Supporting Information (Figs. S2, S3, S10). For deposition reactions by DCS, eliminating H<sub>2</sub> as a by-product has a higher enthalpic barrier (shown in Fig. S17) than eliminating HCl as a by-product (shown in Fig. S1). Therefore, it is determined that the relevant DCS deposition reaction eliminates HCl as a by-product.

In Fig. 1, the reaction pathway A1–A2–A3 shows epitaxial growth on the Si surface. Pathway A1–A4–A1 shows the passivation and reactivation cycle of the Si surface, where passivation involves chlorination of the surface and reactivation is the removal of the chlorine. Similarly, in Fig. 2, pathway B1–B2–B3 shows amorphous silicon growth on the SiO<sub>2</sub> surface. Pathway B1–B4–B5 shows the passivation and reactivation of this surface. B5–B6 show the reactivity of the reactivated surface since it cannot reverse back to the state prior to passivation.

In Fig. 2, it is worth noting that each reaction step on the SiO<sub>2</sub> surface involves gas phase reactants. This is because the reactive sites, which are the surface OH groups, are far from each other; an adsorbed Si atom is about 5 Å away from the nearest surface OH group.

Studying the free energy landscapes for reactions on the c-Si surface reveals that the surface is not adversely affected by side reactions. As can be seen in Fig. 3a, the epitaxial growth pathway A1–A2–A3 has a higher free energy barrier to the side reaction pathway A1–A4–A1 where the surface is passivated by HCl, only to be reduced back to its initial state by DCS. Therefore, we can ignore the A1–A4–A1 pathway and only consider epitaxial growth reactions when comparing to reactions on the SiO<sub>2</sub> surface.

While there is only one relevant reaction route on the c-Si surface, there are several on the SiO<sub>2</sub> surface that contribute towards growth: B1–B2–B3 (growth), B1–B4–B5 (growth on the passivated surface) and B1–B4–B6 (reactivation of the passivated surface), as these reactions have similar free energy barriers. The second and third pathways result in hindered amorphous growth while the first leads to facile amorphous growth. The transition states from B4 to B5 (TSB2b), from B4 to B6 (TSB2c) and other transition states and surface geometries are shown in Figs. S17–S29. From the free energy landscape, several interesting observations can be made. First, the low free energy of B4 indicates that the surface is highly prone to passivation, not only due to the low entropic cost for adsorbing HCl but also due to the high entropic gain from forming H<sub>2</sub>O, a by-product that is not present in the gas flow. Second, it is evident that for all reactions, the second step is rate limiting due to the entropic cost of adsorption of a second molecule.

When growth-related reactions (all reactions except for A1–A4–A1) are compared side by side this conclusion becomes apparent. The calculated energy landscapes show that the free energy cost is due primarily to adsorption of gas phase molecules. As a result, epitaxial growth on Si has a low barrier as compared to the amorphous growth reactions on SiO<sub>2</sub>, which involves a second gas phase reactant molecule. The rate-limiting step on Si is therefore the first step, of DCS deposition, with a barrier of 3.19 eV. On SiO<sub>2</sub>, the second step is always rate limiting, with a barrier of 5.56 eV for amorphous growth, 3.31 eV for reactivating the HCl passivated surface, and 3.30 eV for deposition on a

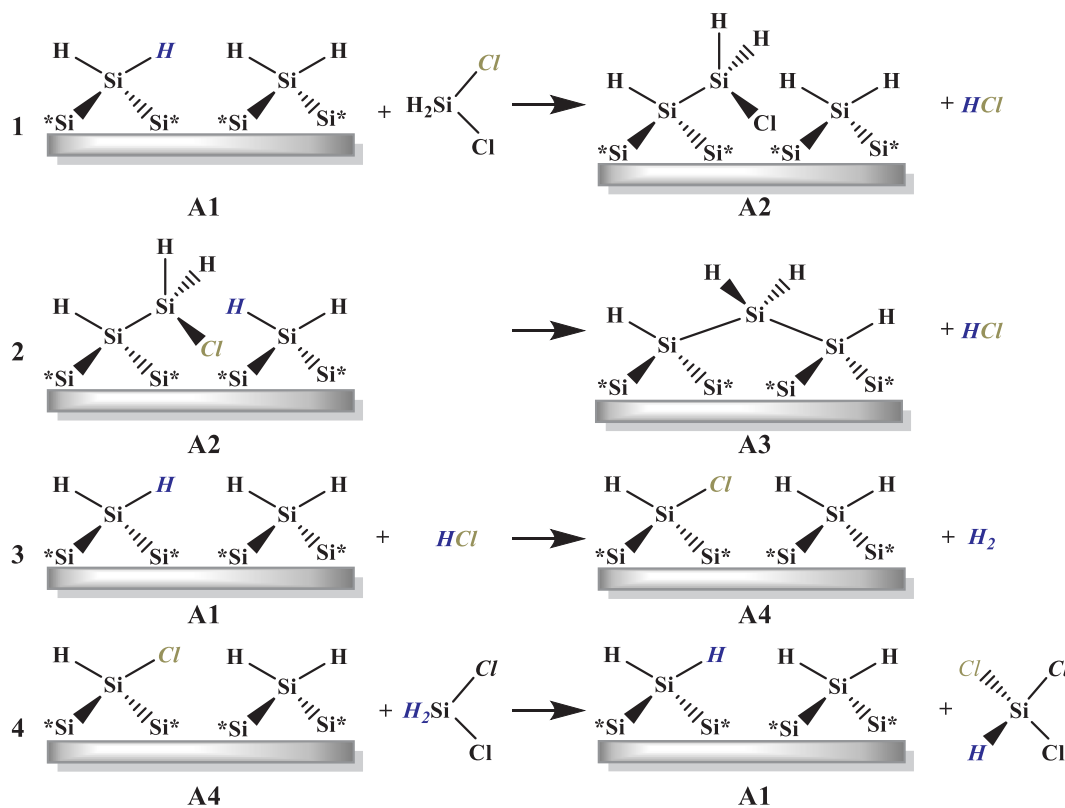


Fig. 1. SEG reactions on the *c*-Si surface. Si\* on the silver bar represents surface silicon of the bulk. A1 is the starting surface. Structure A4 is the inactive Cl passivated surface. Structures A1 to A3 show the two-step epitaxial growth mechanism.

HCl passivated surface. The barrier for SEG is the lowest among all growth-related reactions. This is only somewhat higher than the experimental activation energy for DCS of around 2.5 eV.7, [10].

This difference in barriers between deposition on Si and SiO<sub>2</sub> suggests a higher rate of growth on Si than on SiO<sub>2</sub>. The difference in the free energy barriers is primarily entropic. A decomposition of the free energy profiles due to translational entropy, vibrational entropy, total entropy, and enthalpy for epitaxial growth on *c*-Si and amorphous growth on SiO<sub>2</sub> can be found in Figs. S31 and S32.

This entropic difference arises from an important feature of SEG: on the *c*-Si surface, for every molecule of DCS consumed, two HCl molecules are released into the gas phase, resulting in a net gain of three translational degrees of freedom. This entropy gain of 2 eV drives the endothermic reaction, resulting in an overall free energy near zero. This suggests that SEG is barely a spontaneous process and is consistent with the fact that SEG needs to be driven by low pressure and high temperature. In comparison, the free energy change is +0.79 eV for amorphous growth on SiO<sub>2</sub>, +0.15 eV for deposition on the HCl passivated SiO<sub>2</sub> surface and −2.54 eV for reactivation of the DCS passivated SiO<sub>2</sub> surface. The latter two reactions have lower free energies because of the entropic contribution of the TCS and water by-products. Never-the-less, the entropic contribution of HCl makes SEG favorable thermodynamically.

It's clear that both thermodynamics and kinetics favor epitaxial growth on *c*-Si over SiO<sub>2</sub>. There are, however, other contributing factors. On the SiO<sub>2</sub> surface, there are competing reactions that hinder the first deposition step by DCS. HCl incorporation into SiO<sub>2</sub> (B1–B4) has a low free energy barrier and a significant free energy reduction, due primarily to the low entropy cost of HCl adsorption and the entropy gain associated with releasing water as by-product to the anhydrous environment. This implies that the SiO<sub>2</sub> surface is easily passivated. As a result, the deposition of the first Si group has an elevated barrier at 3.30 eV compared to the amorphous growth mechanism where Si

deposition takes place in the first step with a barrier of 2.70 eV. This mechanism could also contribute to the selectivity of Si epitaxial growth by hindering the initial nucleation step.

From our results, we can suggest that future research should focus on silane with two substituted groups, such as SiH<sub>2</sub>R<sub>2</sub>, to have an overall deposition reaction that releases two high entropy gas phase byproducts per deposited silicon. The byproduct entropy is able to compensate for the high enthalpic barrier of deposition and facilitate epitaxial growth. To improve selectivity, it would be desirable for the substitution groups to have a pacifying effect, such as Cl. Two hydrogen groups are necessary because, as shown above, the surface is terminated with SiH<sub>2</sub>. The silicon precursor forms two Si-Si bonds, each eliminating one substitution group. After this, the newly deposited Si should be terminated with two hydrogen atoms for the growth to be epitaxial. Precursors with more than two halogens should be avoided. For example, TCS leaves Cl on the surface after the two-step deposition. A residual ligand could slow the overall growth because, as shown above, a halogenated surface is less reactive and requires an extra activation step before further deposition.

#### 4. Conclusion

Through analyzing reaction free energy landscapes, the mechanism of SEG on *c*-Si as compared to SiO<sub>2</sub> is explained. Computations illustrate high activation energy barriers for the deposition, illustrating the necessity of high temperature for the process. The rate-determining step for epitaxial growth on single crystal Si is the initial DCS deposition step, with a free energy barrier of 3.19 eV. The second growth step is fast and results in an overall free energy reduction for this two-step reaction. The high barrier is due to the entropy cost of DCS adsorption. The second step has a low barrier because it is a surface reaction that does not involve adsorption of a reactant molecule. The release of by-products into the gas phase results in an entropy gain, which drives this

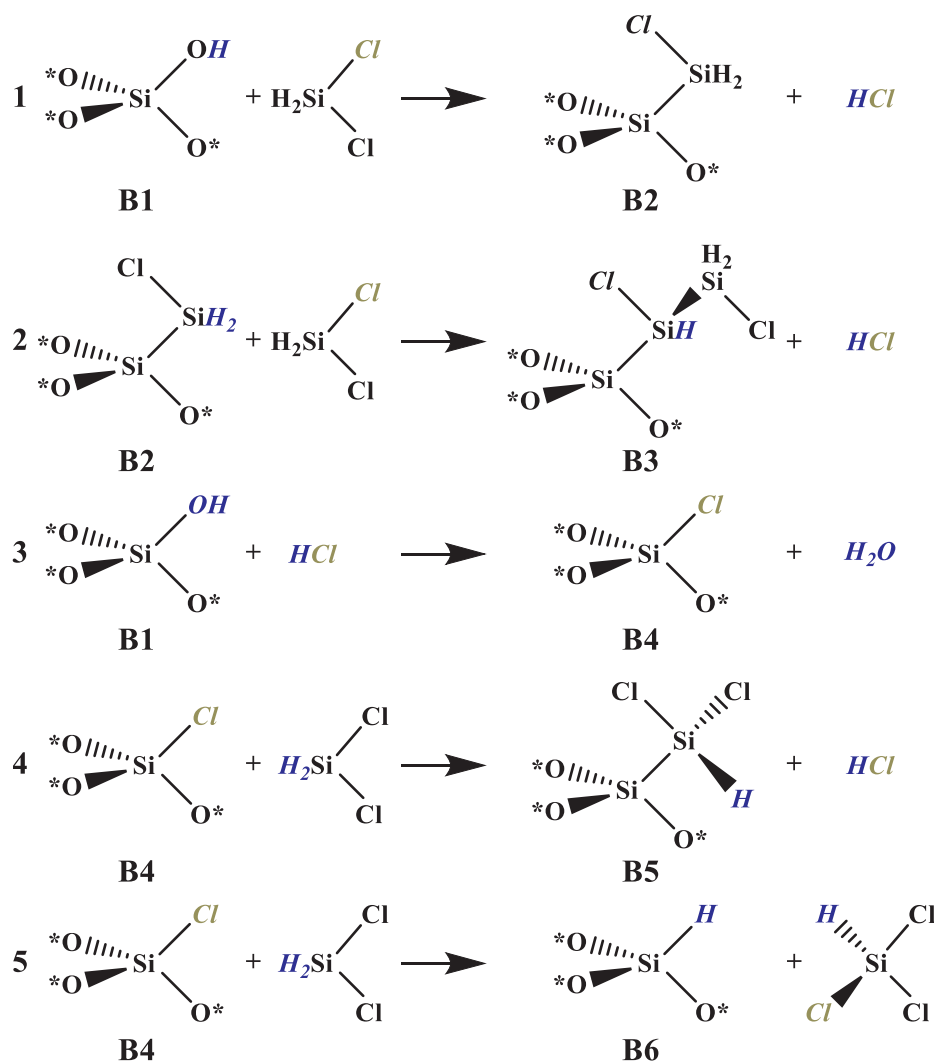


**Fig. 2.** SEG reactions on the SiO<sub>2</sub> surface. B1 is the initial surface. B1 to B3 show the mechanism for direct amorphous growth. B4 is the inactive Cl passivated surface. B5 and B6 show the deposition and reactivation products from B4. SEG is not epitaxial on SiO<sub>2</sub>, but rather amorphous, since the deposited groups do not have the same structure as the sublayers.

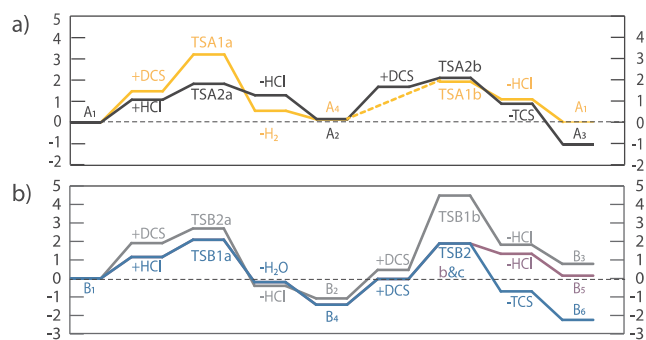


**Fig. 3.** (a) Free energy landscapes for reactions on the c-Si surface. (b) Growth related reactions on the SiO<sub>2</sub> surface.

endothermic epitaxial growth reaction. On SiO<sub>2</sub>, the initial deposition has a relative low barrier of 2.70 eV. The amorphous growth step, however, has a high barrier of 5.56 eV and a free energy increase of 0.79 eV due to the entropic cost of consuming DCS. Moreover, the surface is easily passivated by HCl with a free energy barrier of 2.16 eV and a free energy change of  $-1.42$  eV, due primarily to the formation of water in an anhydrous environment. The passivated surface is less active as the deposition barrier is increased to 3.30 eV. The surface is

also difficult to reactivate by DCS, with a barrier of 3.31 eV. Therefore, Si epitaxial growth is selective on c-Si due to higher entropy of the reactants, while growth on SiO<sub>2</sub> is slower and hindered by chloride passivation. To find better silicon precursors with a higher growth rate, future research could focus on SiH<sub>2</sub>R<sub>2</sub> like precursors that produce two high entropy gas phase byproducts.

#### Declaration of Competing Interest

The authors declare that they have no known competing financial interests or personal relationships that could have appeared to influence the work reported in this paper.

#### Acknowledgement

Special thanks to Atashi Basu, Saurabh Chopra and Abhishek Dube for their help and discussions, and to Yubao Liu for her logistical support and oversight. Financial help from Applied Materials Inc. is greatly appreciated. The work in Austin was supported by the U.S. Welch Foundation under award F-1841.

## Appendix A. Supplementary material

Supplementary data to this article can be found online at <https://doi.org/10.1016/j.apsusc.2020.145888>.

## References

- [1] Z. Ramadan, H.M. Abdelmotalib, I.T. Im, Modeling of epitaxial silicon growth from the DCS-H<sub>2</sub>-HCl system in a large scale CVD reactor, *IEEE Trans. Semicond. Manuf.* 31 (3) (2018) 363–370.
- [2] I. Haller, Selective wet and dry etching of hydrogenated amorphous silicon and related materials, *J. Electrochem. Soc.* 135 (8) (1988) 2042.
- [3] A. Miyauchi, Y. Inoue, T. Suzuki, Low-temperature (850 °C) silicon selective epitaxial growth on HF-treated Si (100) substrates using SiH<sub>4</sub>-HCl-H<sub>2</sub> systems, *J. Electrochem. Soc.* 138 (11) (1991) 3480–3483.
- [4] K.E. Violette, M.C. Öztürk, G. Harris, M.K. Sangneria, A. Lee, D.M. Maher, Nucleation and growth of polycrystalline silicon films in an ultra high vacuum rapid thermal chemical vapor deposition reactor using disilane and hydrogen, *MRS Proc.* 343 (11) (1994) 1–5.
- [5] S. Thomas, M. Bauer, M. Stephens, J. Kouvetakis, Precursors for group IV epitaxy for micro/opto-electronic applications, *Solid State Technol.* 52 (4) (2009) 4–9.
- [6] C.E. Morosanu, D. Iosif, E. Segal, Vapour growth mechanism of silicon layers by dichlorosilane decomposition, *J. Cryst. Growth* 61 (1) (1983) 102–110.
- [7] J.M. Hartmann, V. Benevent, J.F. Damlencourt, T. Billon, A benchmarking of silane, disilane and dichlorosilane for the low temperature growth of group IV layers, *Thin Solid Films* 520 (8) (2012) 3185–3189.
- [8] N. Afshar-Hanaii, J.M. Bonar, A.G.R. Evans, G.J. Parker, C.M.K. Starbuck, H.A. Kemhadjian, Thick selective epitaxial growth of silicon at 960°C using silane only, *Microelectron. Eng.* 18 (3) (1992) 237–246.
- [9] J.L. Hoyt, C.A. King, D.B. Noble, C.M. Gronet, J.F. Gibbons, Limited reaction processing: growth of Si<sub>1-x</sub>Gex/Si for heterojunction bipolar transistor applications, *Thin Solid Films* 184 (1990) 93–106.
- [10] W. Zhang, N.S. Lloyd, K. Osman, J.M. Bonar, J.S. Hamel, D.M. Bagnall, Selective epitaxial growth using dichlorosilane and silane by low pressure chemical vapor deposition, *Microelectron. Eng.* 73–74 (2004) 514–518.
- [11] S.K. Lee, Y.H. Ku, T.Y. Hsieh, K. Jung, D.L. Kwong, Selective epitaxial growth by rapid thermal processing, *Appl. Phys. Lett.* 57 (3) (1990) 3–6.
- [12] M. Shinriki, K. Chung, S. Hasaka, P. Brabant, H. He, T.N. Adam, D. Sadana, Gas phase particle formation and elimination on Si (100) in low temperature reduced pressure chemical vapor deposition silicon-based epitaxial layers, *Thin Solid Films* 520 (8) (2012) 3190–3194.
- [13] T.N. Adam, S. Bedell, A. Reznicek, D.K. Sadana, A. Venkateshan, T. Tsunoda, T. Seino, J. Nakatsuru, S.R. Shinde, Low-temperature growth of epitaxial (1 0 0) silicon based on silane and disilane in a 300 Mm UHV/CVD Cold-wall reactor, *J. Cryst. Growth* 312 (23) (2010) 3473–3478.
- [14] T.R. Mayangsari, L.L. Yusup, J.M. Park, E. Blanquet, M. Pons, J. Jung, W.J. Lee, Study of surface reaction during selective epitaxy growth of silicon by thermodynamic analysis and density functional theory calculation, *J. Cryst. Growth* 468 (2017) 278–282.
- [15] M. Hierlemann, A. Kersch, C. Werner, H. Schäfer, A gas-phase and surface kinetics model for silicon epitaxial growth with SiH<sub>2</sub>Cl<sub>2</sub> in an RTCVD reactor, *J. Electrochem. Soc.* 142 (1) (1995) 259–266.
- [16] I. Zaidi, Y.H. Jang, D.G. Ko, I.T. Im, Numerical modeling study on the epitaxial growth of silicon from dichlorosilane, *J. Cryst. Growth* 483 (2018) 1–8.
- [17] K.H. Chung, N. Yao, J. Benziger, J.C. Sturm, K.K. Singh, D. Carlson, S. Kuppuraio, Ultrahigh growth rate of epitaxial silicon by chemical vapor deposition at low temperature with neopentasilane, *Appl. Phys. Lett.* 113506 (2008) 6–9.
- [18] G. Kresse, J. Hafner, Ab initio molecular dynamics for liquid metals, *Phys. Rev. B* 47 (1) (1993) 558.
- [19] G. Kresse, J. Furthmüller, Efficiency of ab-initio total energy calculations for metals and semiconductors using a plane-wave basis set, *Comput. Mater. Sci.* 6 (6) (1996) 15–20.
- [20] G. Kresse, J. Furthmüller, Efficient iterative schemes for ab initio total-energy calculations using a plane-wave basis set, *Phys. Rev. B - Condens. Matter Mater. Phys.* 54 (16) (1996) 11169–11186.
- [21] G. Kresse, D. Joubert, From ultrasoft pseudopotentials to the projector augmented-wave method, *Phys. Rev. B* 59 (3) (1999) 1758–1772.
- [22] P.E. Blöchl, Projector augmented-wave method, *Phys. Rev. B* 50 (24) (1994) 17953–17979.
- [23] J. P. Perdew, K. Burke, M. Ernzerhof Generalized Gradient Approximation Made Simple, *Phys. Rev. Lett.* 1996, 77 (18), 3865–3868.
- [24] J.T. Fitch, Selectivity mechanisms in low pressure selective epitaxial silicon growth, *J. Am. Chem. Soc.* E 141 (4) (1994) 1046–1055.
- [25] J.P. Balbuena, I. Martin-bragado, Lattice kinetic Monte Carlo simulation of epitaxial growth of silicon thin films in H<sub>2</sub> / SiH<sub>4</sub> chemical vapor deposition systems, *Thin Solid Films* 634 (2017) 121–133.
- [26] G. Henkelman, B.P. Uberuaga, H. Jónsson, A climbing image nudged elastic band method for finding saddle points and minimum energy paths, *J. Chem. Phys.* 113 (22) (2000) 9901–9904.
- [27] S.A. Trygubenko, D.J. Wales, A doubly nudged elastic band method for finding transition states, *J. Chem. Phys.* 120 (5) (2004) 2082–2094.
- [28] G. Henkelman, H. Jónsson, A dimer method for finding saddle points on high dimensional potential surfaces using only first derivatives, *J. Chem. Phys.* 111 (1999) 7010–7022.
- [29] C.T. Campbell, J.R.V. Sellers, The entropies of adsorbed molecules, *J. Am. Chem. Soc.* 134 (43) (2012) 18109–18115.